DSE-4042-T40

ADVANCED PHOTOVOLTAIC CONCENTRATOR CELLS

Quarterly Technical Progress Report No. 2, December 1, 1979—February 29, 1980

By
S. W. Zehr
H. T. Yang
J. J. Yang
J. S. Harris, Jr.

March 1980

Work Performed Under Contract No. AC02-77CH00178

Rockwell International
Electronics Research Center
Thousand Oaks, California

and

Rockwell International
Electronics Research Center
Anaheim, California

U.S. Department of Energy

Solar Energy

DISCLAIMER

DISCLAIMER

Available from the National Technical Information Service, U. S. Department of Commerce, Springfield, Virginia 22161.

Price: Paper Copy $6.00
Microfiche $3.50

DSE-4042-T40
Distribution Categories UC-63 and UC-63e

March, 1980 ERC41033.17TPR

ADVANCED PHOTOVOLTAIC CONCENTRATOR CELLS

Quarterly Technical Progress Report No. 2
for period 12/1/79 through 02/29/80

By

S. W. Zehr, H. T. Yang, J. J. Yang* and J. S. Harris, Jr.
Rockwell International Electronics Research Center
Thousand Oaks, California 91360
*Anaheim, California 92803

For

Solar Energy Research Institute
Photovoltaics Program Office
PVPO - Documentation
1617 Cole Boulevard
Golden, Colorado 80401

Prepared under Contract No. XJ-9-8058-2

Approved by:

J. S. Harris, Jr.
Program Manager

Rockwell International

TABLE OF CONTENTS

LIST OF FIGURES

ABSTRACT

This report describes second quarter activities for a project aimed at demonstrating the technical feasibility of advanced high efficiency concentrator solar converters. The goal of the program is to achieve 30% conversion efficiency with a converter operating at 30°C under 500-1000 SUN AM2 illumination and 25% conversion efficiency with a converter operating at 150°C under 500-1000 SUN AM2 illumination. The approach is to fabricate two cell, non-lattice matched, monolithic stacked converters using optimum pairs of cells having bandgaps in the range of 1.6-1.7 eV and 0.95-1.1 eV. The high bandgap cells are to be fabricated using MOCVD or LPE to produce the needed AlGaAs layers of optimized composition, thickness and doping to produce high performance, heteroface homojunction devices. The low bandgap cells are to be similarly fabricated from AlGaSb(As) compositions by LPE. These subcells are then to be joined into a monolithic structure by an appropriate thermal bonding technique which will also form the needed transparent intercell ohmic contact (IOC) between the two subcells.

The activities this quarter have been largely focused on the development and study of low bandgap cell structures and attempts to develop suitable techniques for the thermal bonding operation.

1.0 INTRODUCTION

Within the last several years, there has been growing interest in exploiting the significantly improved levels of power conversion efficiency which are theoretically available from multibandgap solar photovoltaic converters[1-5]. This interest has been sparked by the recognition that even a partial realization of these potential performance gains can provide significant leverage for reduction of the cost of output electric power from concentrator photovoltaic systems[6].

Upper bound conversion efficiencies near 40% and 47% have been calculated for optimum bandgap two and three junction converters respectively operating at 300°K under terrestrial sunlight concentrated to several hundred to one thousand SUNs[1-5]. Even when practical losses are taken into account, such converters offer a reasonable prospect for achieving at least 30% efficiency from stacked, monolithic, two-bandgap structures of well-optimized design, operating at 30°C under 500-1000 SUN AM2 illumination.

Such devices also offer the option of operating at these levels of sunlight concentration at moderately elevated temperatures (~150°C) with at least 25% electrical conversion efficiency and the added bonus of providing usable quality heat for total energy applications.

It is the objective of this project to demonstrate the technical feasibility of producing monolithic stacked multibandgap solar cells having 30% conversion efficiency at 30°C and 25% conversion efficiency at 150°C under 500-1000 SUN AM2 illumination.

To meet this objective, the following tasks will be performed:

1. Grow and optimize single junction AlGaAs cells having bandgaps of 1.6 eV and 1.7 eV and AlGaSb cells having bandgaps of 0.95 eV and 1.1 eV.
2. Develop techniques for joining these optimized single junction cells by means of non-lattice matched intercell ohmic contacts

having sufficient optical transparency combined with low electrical and thermal resistance to meet the overall performance objective.

3. Characterize performance of the individual cells and stacked combinations using appropriate light and dark I-V and spectral response measurements over the operating temperature range of 30-200° C and for illumination levels of 1-1000 SUNs AM2.

2.0 MODELING

There was no modeling activity during this quarter. This effort will resume in the next quarter and will largely consist of matching calculated spectral response curves and integrated short circuit current densities with measured values. Such matching will provide estimates of minority carrier diffusion lengths for comparison with values measured by such techniques as EBIC. The combined results from measurement and calculation will serve as the basis for re-optimization of subcell and converter design.

3.0 MATERIALS DEVELOPMENT

3.1 Accomplishments

- A wide range of AlGaSb structures related to the ultimate subcell structures have been produced and partially evaluated.
- Initial MOCVD AlGaAs inverted subcell structures have been produced. Work is underway to develop suitable GaAs substrate removal techniques.
- The LPE AlGaAs structures for ITO ohmic contact studies have been supplied to Raj Singh at Colorado State University. Initial ITO layers have been deposited on some of the wafers but are of rather poor quality.
- Successful bonding of GaAs to GaSb has been accomplished with an AlSb bonding layer formed in-situ by transient melting and reaction of thin predeposited layers of elemental Al and Sb.
- An initial problem of delineating p-n junctions in AlGaSb by etching cleaved cross-sections has been overcome.

3.2 Substrates

3.2.1 GaSb Substrates

The GaSb boule needed to supply substrates for this program has been grown and partially processed into wafers. This boule is expected to supply sufficient substrates for the remainder of phase 1 of this program.

3.2.2 GaAs Substrates

In addition to our existing supply of GaAs wafers from commercial sources, we will from time to time be using material produced from large

diameter boules grown in-house in our recently acquired MRC crystal puller.

3.3 AlGaAs Subcells

An initial AlGaAs subcell structures has been produced by MOCVD. The structure is that shown schematically in Fig. 3.1. In this case, the subcell structure has been grown inverted (window layer first) to allow direct bonding of the last grown n-$Al_{.2}Ga_{.8}As$ layer to the underlying AlGaSb subcell structure. After bonding, the GaAs substrate is to be removed from the assembly to allow direct access of the incident illumination to the $Al_{.85}Ga_{.15}As$ window layer.

Extensive work with this structure aimed at developing substrate removal techniques indicates that the 600Å $Al_{.85}Ga_{.15}As$ window layer is too thin to reliably withstand exposure to the pH-controlled H_2O_2 etch used to selectively dissolve the GaAs. Because of difficulties in maintaining precise parallelism between the substrate/window interface and the wafer surface during lapping, the window layer becomes unevenly exposed during substrate dissolution. While the rate of dissolution of the AlGaAs is perhaps an order of magnitude or two slower than that of the overlying GaAs, the several additional minutes of exposure to the etching solution needed for complete removal of the remainder of the GaAs often results in complete dissolution of the initially exposed AlGaAs regions.

After considerable effort to overcome this problem by more careful technique, it appears now that the most practical solution is to simply grow two additional layers consisting of ~0.5 to 1 μm of AlGaAs followed by ~1-2 μm of GaAs prior to growth of the thin window subcell structure. With these additional layers, it should be possible to completely remove the GaAs substrate with existing lapping and etching techniques without undue risk of penetrating the thicker additional AlGaAs layer. Once this has been accomplished, an HF based etch can be used to selectively dissolve the added AlGaAs from the underlying GaAs layer. This GaAs layer can then

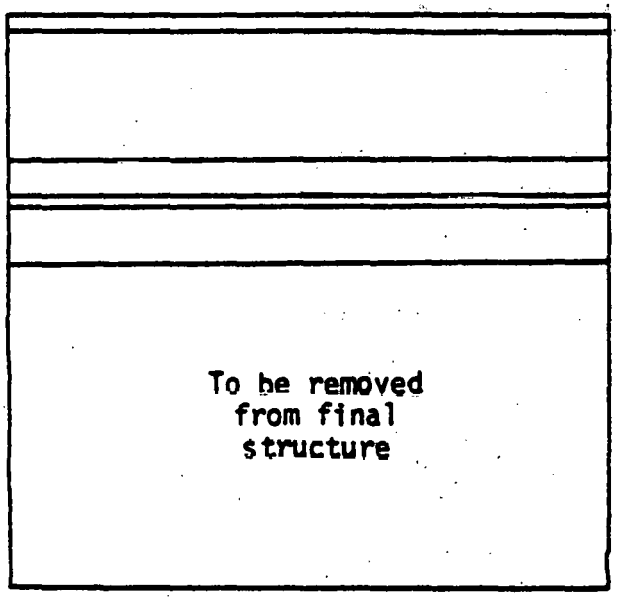

0.1 μm n^+ $Al_{.2}GaAs$

4.0 μm n $Al_{.15}GaAs$

0.5 μm p $Al_{.15}GaAs$

~600Å p $Al_{.85}GaAs$

1.5 μm p GaAs (buffer)

p^+ GaAs Substrate

Fig. 3.1 Schematic layer structure for high bandgap AlGaAs subcell grown inverted to allow GaAs substrate removal after bonding to low bandgap subcell.

either be removed completely, or be made heavily p-doped and pattern etched through photoresist to provide a low resistance base for easily forming the needed front surface contact grid. Initial MOCVD growth of large areas of this type of structure is scheduled for early in the next quarter. The compositional and layer thickness details will be adjusted to include changes leading to better performance which are suggested by the latest modeling and measurement of spectral response curves.

3.4 AlGaSb Subcells

Growth efforts have centered on development of low bandgap heteroface subcells with the structure: p^+ $Al_{.65}Ga_{.35}AsSb$/p $Al_{.2}Ga_{.8}Sb$/n $Al_{.2}Ga_{.8}Sb$/n GaSb. Because of a shortage of Te-doped GaSb polycrystal, we have begun to use Te-doped InSb as the n-type dopant source.

Several p^+ $Al_{.65}Ga_{.35}Sb(As)$ layers have been grown either directly on n-GaSb (100) substrates or in a few cases on p-n $Al_{.2}Ga_{.8}Sb$ junction layers. The addition of As is intended to partially compensate the modest ($\sim$0.7%) difference in lattice parameter between the Al-rich and Ga-rich alloys. Because of limited As solubility at the growth temperature of $\sim$510°C, it is not possible to completely compensate the lattice parameter difference using As.

During this series of growths, frequent problems have been encountered with either poor wetting and nucleation, particularly by the 65% Al layer, or etchback of underlying layers at various stages of growth. The first problem is believed to be associated with oxidation. Some improvement in window layer quality has been achieved by reducing the Al content in the window from 65% to 40%. While this gives too low a bandgap for use in the ultimate subcell application, it does allow growth of interim structures which can yield useful performance information. In an effort to achieve better growths at the 65% Al level, we are in the process of thoroughly cleaning and leak checking the entire growth system.

Accumulated evidence from several growths suggests that the presence of As might be responsible for the observed etchback problems. Subsequently, it has been found that fairly smooth layers of $Al_{.65}Ga_{.15}Sb$ can be grown directly on the GaSb substrate. A photomicrograph of typical growth morphology appears in Fig. 3.2. We will attempt to reproduce this improved window layer quality in growths on p-n $Al_{.2}Ga_{.8}Sb$ layers during the coming quarter.

A problem of p-n junction delineation has been encountered for the $Al_{.2}Ga_{.8}Sb$ alloy. The conventional A-B etch used for many III-V compounds gave unsatisfactory results for this alloy. The problem was eventually overcome by following a suggestion by David Law, of our laboratory, that a 10:1 dilution of the standard AB etch be used and the etching time be limited to <2 sec.

A problem of producing low resistance ohmic contacts to the AlGaSb subcells recently came to light during preliminary attempts to measure illuminated I-V curves under moderate concentration (35-40 SUNs). We are pursuing or planning several activities to develop the needed low resistance contacts.

3.5 Intercell Ohmic Contacts (IOCs) and Bonding

3.5.1 In-Situ Formation of IOC and AlSb Window During Bonding

During the past quarter we have demonstrated successful formation of an AlSb window layer and ohmic contact junction region between bonded wafers of GaSb and GaAs. These bonds have sufficient metallurgical and mechanical integrity to allow the resulting assembly to be monolithically cleaved in cross section without separation across the bonded region.

The successful bonding procedure involves MBE deposition of successive layers of ~ 1 μm of Al and ~ 2 μm of Sb on wafers of both GaAs and GaSb. The relative thicknesses of these elemental layers are such that a region of stoichiometric AlSb can be formed by their complete reaction.

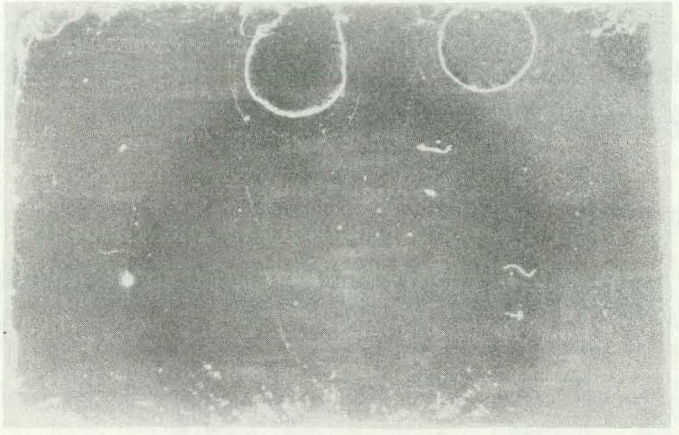

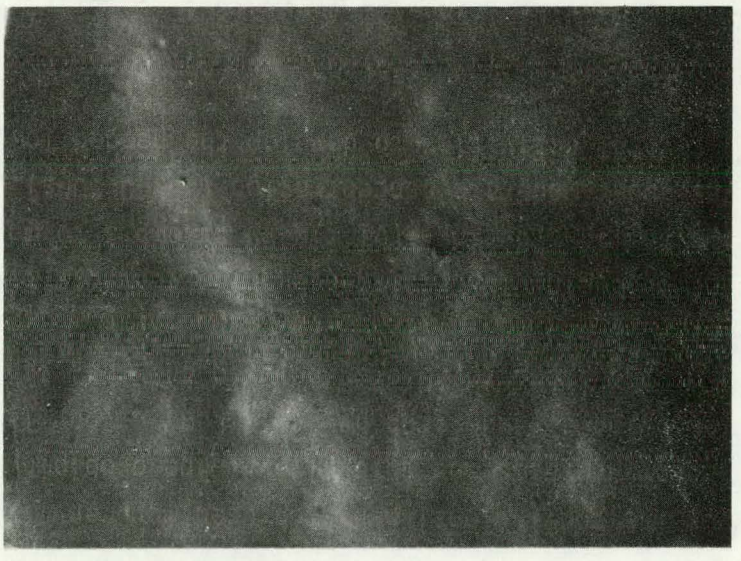

Fig. 3.2 Typical growth morphology of an Al. Ga. Sb layer grown directly on a (100) GaSb substrate. (a) 7X magnification, (b) 400X magnification.

In the initial runs following deposition of the Al layer, the wafers had to be transferred to a second MBE machine for the Sb deposition. These samples were exposed to air during this transfer. To remove the oxide layer thus formed, the Al surfaces were sputter cleaned in the second MBE chamber prior to the Sb deposition. The before and after Auger traces shown in Fig. 3.3 indicate virtually complete removal of oxygen from the Al surface during the sputtering.

The actual bonding involves the transient local melting of the elemental Al and Sb layers to allow mixing and in-situ reaction to form AlSb. A thermal gradient is maintained across the assembly during the bonding operation by heating from the GaAs side only. The bond region can thus be heated slightly above the elemental melting points of Al and Sb (660° C and 630° C respectively) without danger of reaching the 710° C melting point of the GaSb substrate. (The melting point of the GaAs substrate is 1238° C, a value sufficiently high to withstand the needed thermal cycle.) The AlSb reaction product has a melting point of ~1050° C, thus directly producing a solid on reaction at the bonding temperature.

The AlSb has nearly the same lattice parameter as the underlying AlGaSb alloy composing the low bandgap subcell structure. This facilitates its epitaxial growth after nucleation on the p-layer of AlGaSb. The interface thus formed should have the low defect density and carrier recombination velocity needed to ensure good carrier collection in the lower subcell. Because of the imposed temperature gradient during bonding, the AlSb solidification front moves from the AlGaSb surface toward the overlying AlGaAs high bandgap subcell structure. When it finally reaches the AlGaAs, the resulting interface is not epitaxial or lattice-matched. There is generally crystallographic misorientation, as well as an ~8% mismatch of lattice parameters across this interface, leading to a high density of crystallographic defects. Further contributing to this locally high defect density are the chemical impurities which have been swept out of the bond region

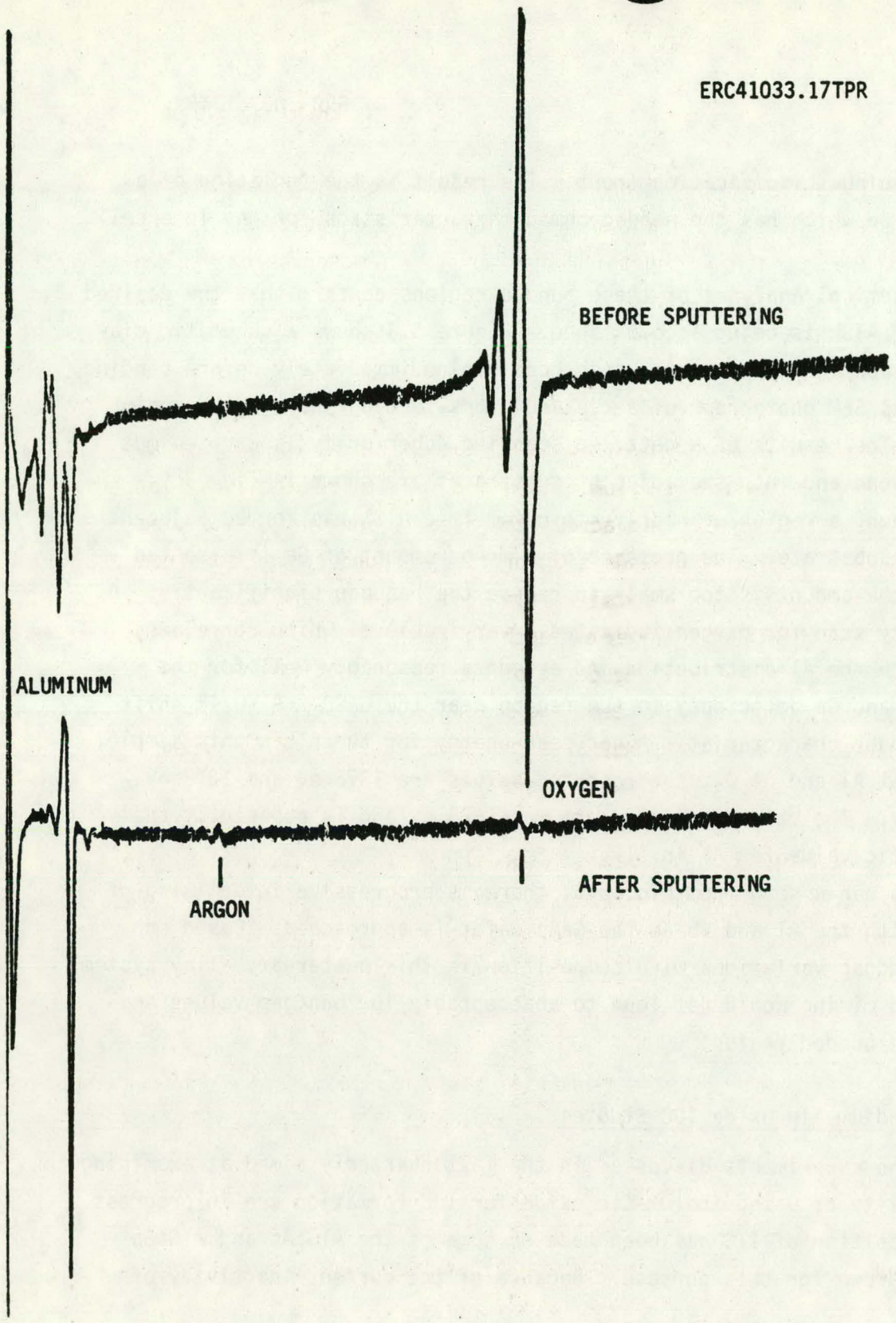

Fig. 3.3 Auger traces of MBE grown Al bonding layer before and after sputter cleaning to remove oxide.

by the advancing solidification front. The result is the formation of a heterojunction which has the needed ohmic characteristics for the intercell contact.

Chemical analyses of these bonded regions confirm that the desired formation of AlSb is being accomplished. Figure 3.4 shows a schematic diagram of the configuration of one such bond region immediately before bonding and a typical SEM photograph of a cleaved cross-section through the region afterward. The results of a detailed scanning Auger analysis carried out across the bond and into the adjacent substrates are shown in Fig. 3.5. As can be seen, a region of nearly stoichiometric AlSb has formed adjacent to the GaSb substrate. The presence of a minor amount of Ga is also indicated, but the amount is too small to reduce the bandgap significantly. A supplementary scan for oxygen indicated a varying level which correlates directly with the Al distribution and accounts reasonably well for the apparent Al and Ga deficiency in the region near the GaSb. A small shift was found in the characteristic Auger peak energy for the Al in this sample. For elemental Al and Al_2O_3, the reported values are 1396 eV and 1378 eV, respectively. The value measured here was 1385 eV and is apparently the characteristic value for Al in AlSb.

As can be seen from Fig. 3.5, there is progressive intermixing of Ga and As with the Al and Sb as the GaAs wafer is approached. Based on reported bandgap variations with composition in this quaternary alloy system, the observed mixing would not lead to unacceptably low bandgap values anywhere in the bonded region.

3.5.2 Indium Tin Oxide IOC Studies

The experiments discussed in the last quarterly aimed at examining the feasibility of using indium-tin oxide for IOC formation are in progress. Initial deposition of ITO has been made on some of the AlGaAs and AlGaSb structures grown for this purpose. Because of the current inactivity of

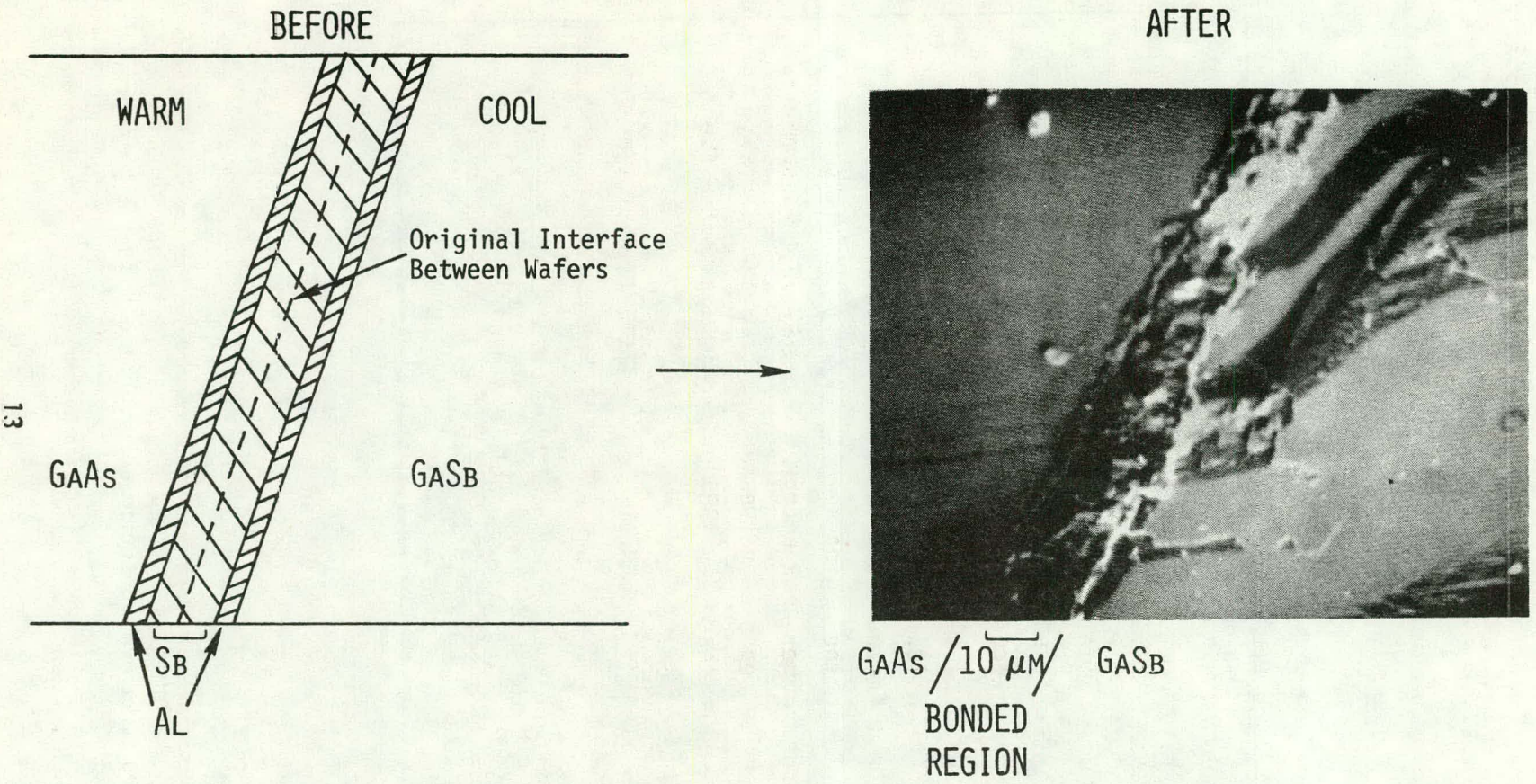

Fig. 3.4. Schematic diagram of as deposited elemental Al and Sb bonding layers prior to bonding and a typical SEM photograph of a cleaved cross-section through the region after bonding.

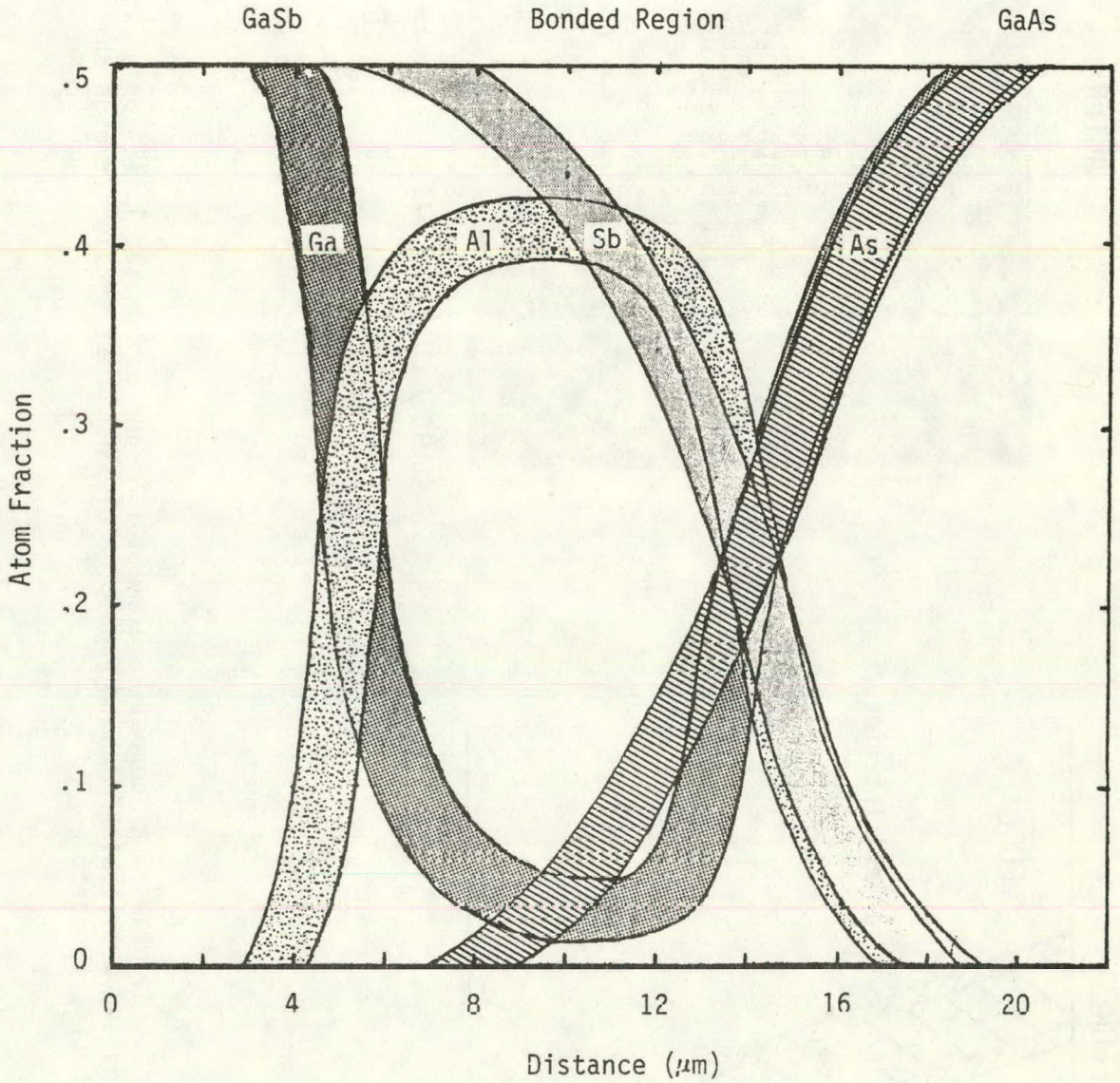

Fig. 3.5 Plot of elemental concentration vs. distance through bond region obtained in scanning Auger analysis.

the DC sputtering system at the Stanford Materials Science Lab, the ITO deposition is being done at Colorado State University by Raj Singh.

Visually, the quality of some of the initially deposited layers is not very good. It appears that improved cleaning procedures may be required. This activity will be pursued further in the coming quarter.

3.5.3 Laser Bonded IOC Structures

The Nd-glass laser to be used in the last bonding experiments is scheduled to be delivered by the end of June.

4.0 DEVICE FABRICATION AND CHARACTERIZATION

4.1 Accomplishments

- The determination of doping levels in AlGaSb layers by differential capacitance-voltage measurements has begun.
- Initial determination of p-n junction location and diffusion length estimates have been made using EBIC measurements.
- Subcell devices have been fabricated from AlGaSb and measurements made of their illuminated and dark I-V and spectral responses.
- I-V measurements of bonded assemblies of n-GaSb/in-situ grown AlSb/n-GaAs have demonstrated ohmic behavior across the bonded region.

4.2 AlGaSb Subcells

4.2.1 Material Characterization

We have begun detailed characterization of doping levels and minority carrier diffusion lengths in AlGaSb layers and structures. Determination of doping levels in LPE grown AlGaSb layers is being done using differential capacitance-voltage measurements. A typical set of results for an n-$Al_{.2}Ga_{.8}Sb$ (Te-doped) layer grown on a (100) n-GaSb substrate is shown in Fig. 4.1. The indicated doping level of 3×10^{17} is in the range of interest, through perhaps not optimum for the present application. Work will continue during the coming quarter to explore the range of achievable dopings and their correlation with growth parameters for the AlGaSb(As) alloy system.

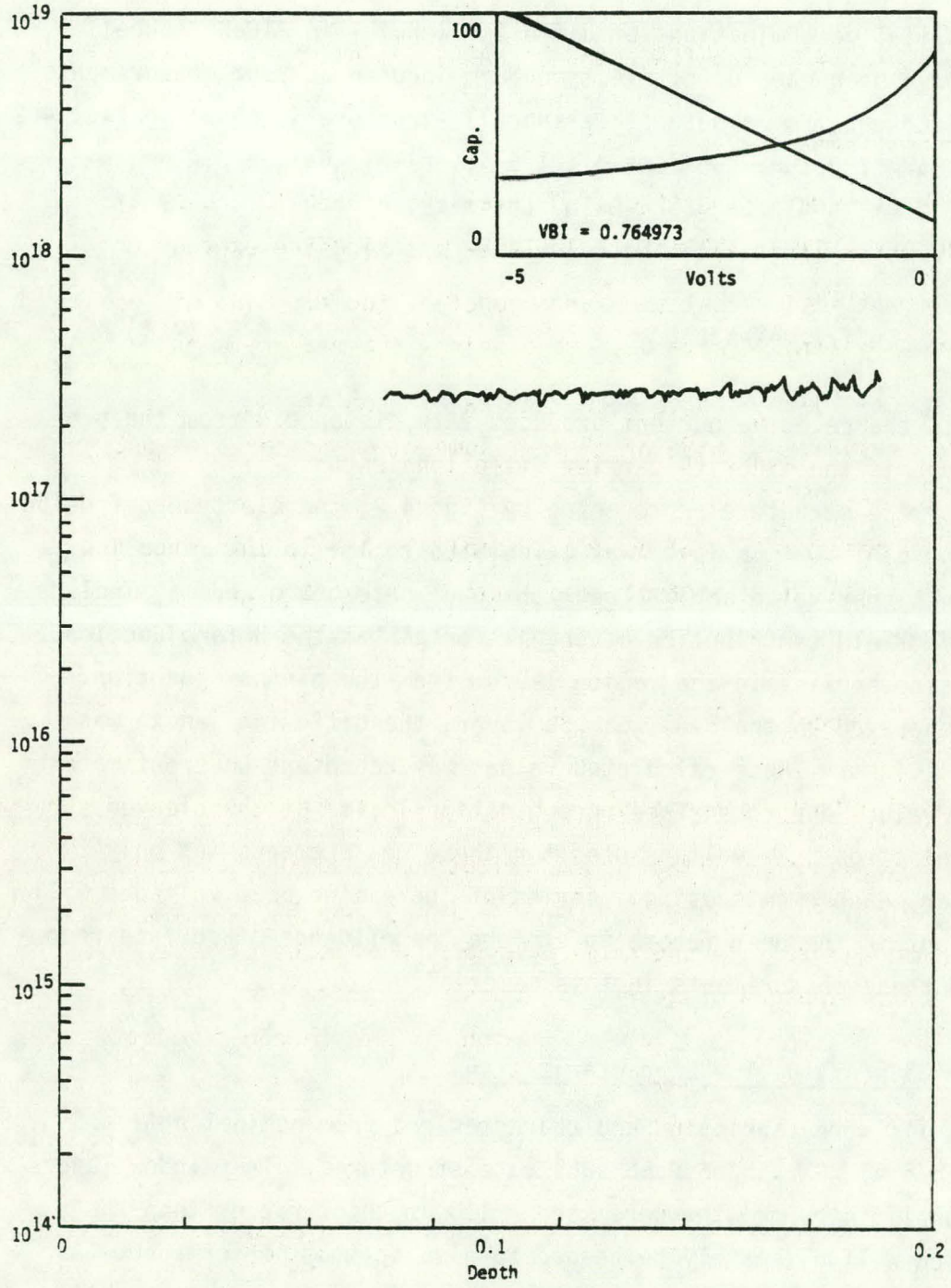

Fig. 4.1 Typical results of doping level determination by means of differential C-V measurements. Sample is an n-$Al_{.2}Ga_{.8}Sb$ layer grown by LPE on a (100) n-GaSb substrate. Te is the n dopant.

Initial determinations of diffusion lengths in AlGaSb subcell structures have been made using electron-beam-induced current measurements. A typical EBIC scan from a heteroface subcell structure is shown in Fig. 4.2. This particular structure consists of: 1.5 μm, p^+-$Al_{.4}Ga_{.6}Sb$/3.4 μm, p-$Al_{.2}Ga_{.8}Sb$/5.0 μm, n-$Al_{.2}Ga_{.8}Sb$/n-GaSb substrate.

Diffusion lengths can be calculated assuming the expression:

$$\ell n\ I/I_o = -X/L \qquad (4.1)$$

where I/I_o is the relative current produced at a distance x from the p-n junction and L is the minority carrier diffusion length.

For the structure represented by Fig. 4.2, the electron diffusion length in the p-$Al_{.2}Ga_{.8}Sb$ layer was calculated to lie in the range 1.4 - 1.6 μm. The higher value applies near the p-p^+ heteroface and may include a local drift field contribution having its origin at the heterojunction. The lower value applies in the region 1-2 μm from the p-n homojunction. For holes generated in the n-$Al_{.2}Ga_{.8}Sb$ layer, the diffusion length was found to be 1.4 μm. These calculated values may represent underestimates of the true values due to surface recombination losses at the cleaved surface. The electron beam voltage used for these measurements was only 20 keV. Further measurements using a series of increasing beam voltages will be carried out in the near future to explore the influence of surface recombination on these measurements in this material.

4.2.2 AlGaSb(As) Device Characterization

Cells were fabricated and characterized from nominal p $Al_{.65}Ga_{.15}Sb$/ p $Al_{.2}Ga_{.8}Sb$/n $Al_{.2}Ga_{.8}Sb$/n^+ GaSb substrate structures. The window layers for these preliminary growths were made ~1.0 μm thick rather than the ~1000Å which will ultimately be needed to give optimum performance. As a result, the measured short circuits are below those thought to be ultimately achievable. Also contributing to the low value of measured current is the

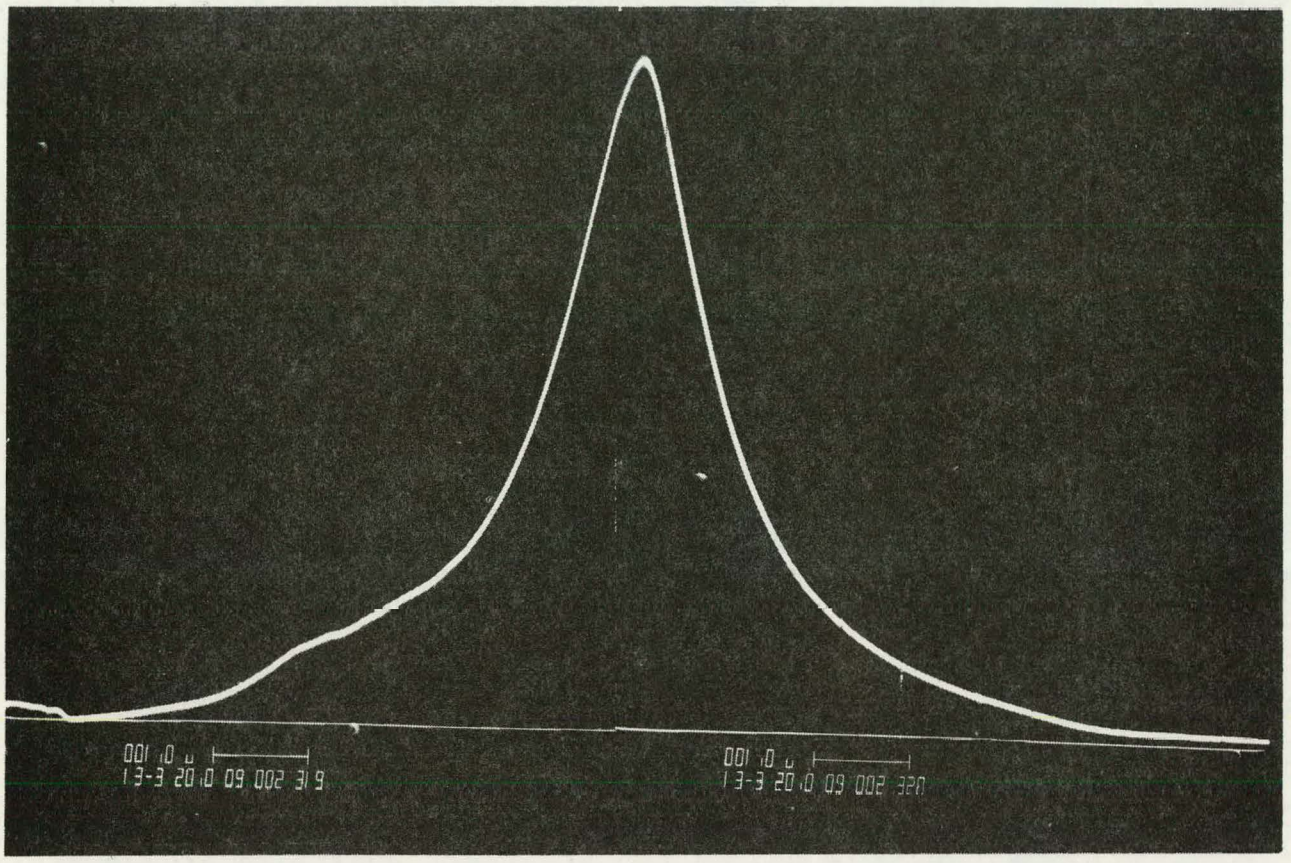

Fig. 4.2 Typical plot of relative electron beam induced current intensity vs. position in an AlGaSb heteroface subcell structure. Structure is: 1.5 μm p^+ $Al_{.4}Ga_{.6}Sb$/3.5 μm p $Al_{.2}Ga_{.8}Sb$/5.0 μm n $Al_{.2}Ga_{.8}Sb$/n GaSb substrate.

fact that the ELH lamps in our simulator utilize a "cold" dichroic mirror reflector which yields a relatively low output in the infrared spectral region utilized by this type of cell. Typical AM1 results are V_{oc} = 0.29 volt, $J_{sc} = 7 \times 10^{-3}$ amp/cm^2, and F.F. = 0.45.

Work is underway to correlate the measurements made using the simulator with those made in natural sunlight.

The diode quality of these initial structures was rather poor indicating some shunting of the junctions. A typical spectral response curve for one of these devices is shown in Fig. 4.3. It indicates that the layer compositions actually produced are essentially those intended. The window long wavelength cutoff occurs in the range ~0.8 - 0.95 μm, consistent with an AlSb mole fraction of about 0.65. The p-n junction cutoff occurs at about 1.3 μm (0.95 eV) as would be expected from a composition having an AlSb mole fraction of 0.20.

Cells were also fabricated and characterized from the structures having the window layer Al content reduced to 40%. Fig. 4.4 shows a typical dark log I-V curve from a typical device having the structure: p-$Al_{.4}Ga_{.6}Sb$ 1.7 μm/p-$Al_{.2}Ga_{.8}Sb$ 3.4 μm/n-$Al_{.2}Ga_{.8}Sb$ 5 μm/n-GaSb substrate. The saturation current density, J_o, is 5.2×10^{-5} A/cm^2. The diode factor, n, is 2.7. Figure 4.5 shows the light I-V curve for the same device under simulated 1 SUN AM1 illumination. As indicated, V_{oc} = 0.317, J_{sc} = 6.9 mA/cm^2 and F.F. = 0.514. When the intensity of illumination was increased to 35 SUNs, the illuminated I-V curve of Fig. 4.6 was obtained. As can be seen, the V_{oc} increased markedly to 0.445 volt. This strong sensitivity of V_{oc} to light intensity is to be expected from relatively low bandgap structures having relatively large J_o's. The problem of high series resistance encountered with these early devices is also quite evident from the shape of the I-V curve in this figure and the indicated F.F. = 0.23.

A typical spectral response curve for this structure is shown in Fig. 4.7. It is qualitatively similar to that shown in Fig. 4.3 except that the short wavelength cutoff occurs at a longer wavelength with the 40% total window layer than with 65% Al.

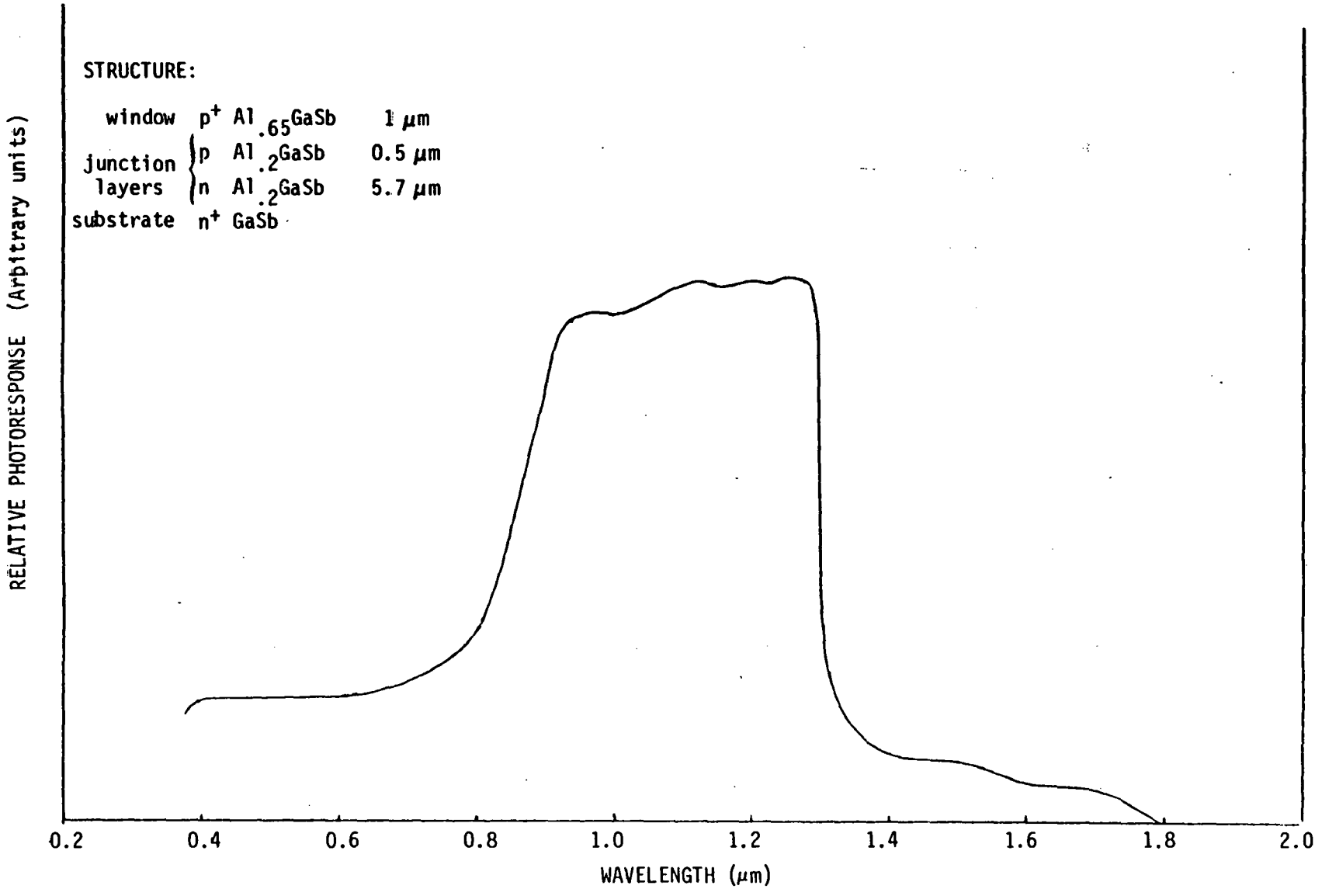

Fig. 4.3. Relative spectral response from a p^+ $Al_{.65}Ga_{.35}Sb/p$ $Al_{.2}Ga_{.8}Sb/n$ $Al_{.2}Ga_{.8}Sb/n^+$ GaSb low bandgap subcell structure.

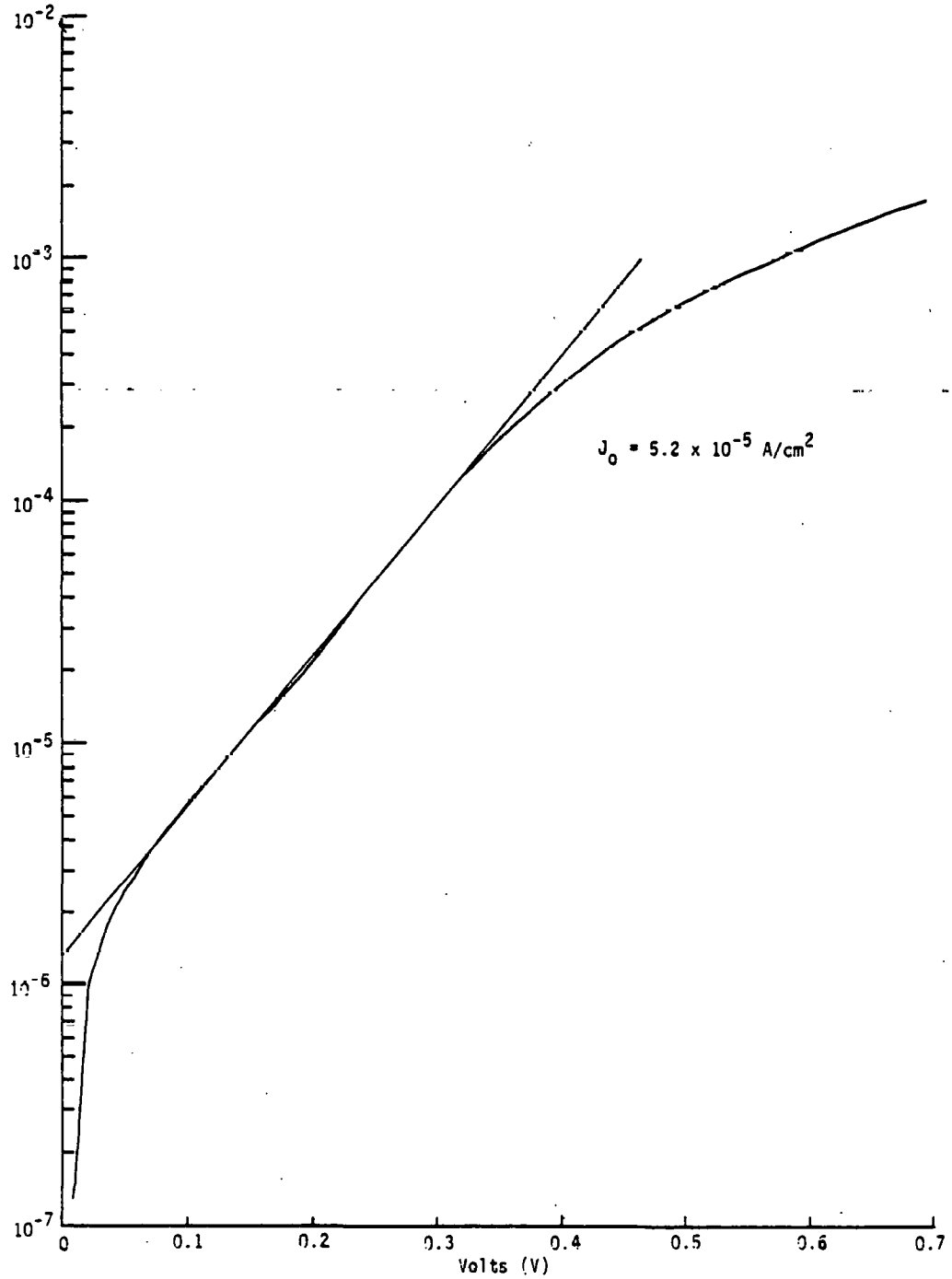

Fig. 4.4 Typical dark log I-V curve for a p^+ $Al_{.4}Ga_{.6}Sb/p$ $Al_{.2}Ga_{.8}Sb/n$ $Al_{.2}Ga_{.8}Sb/n^+$ GaSb low bandgap subcell structure.

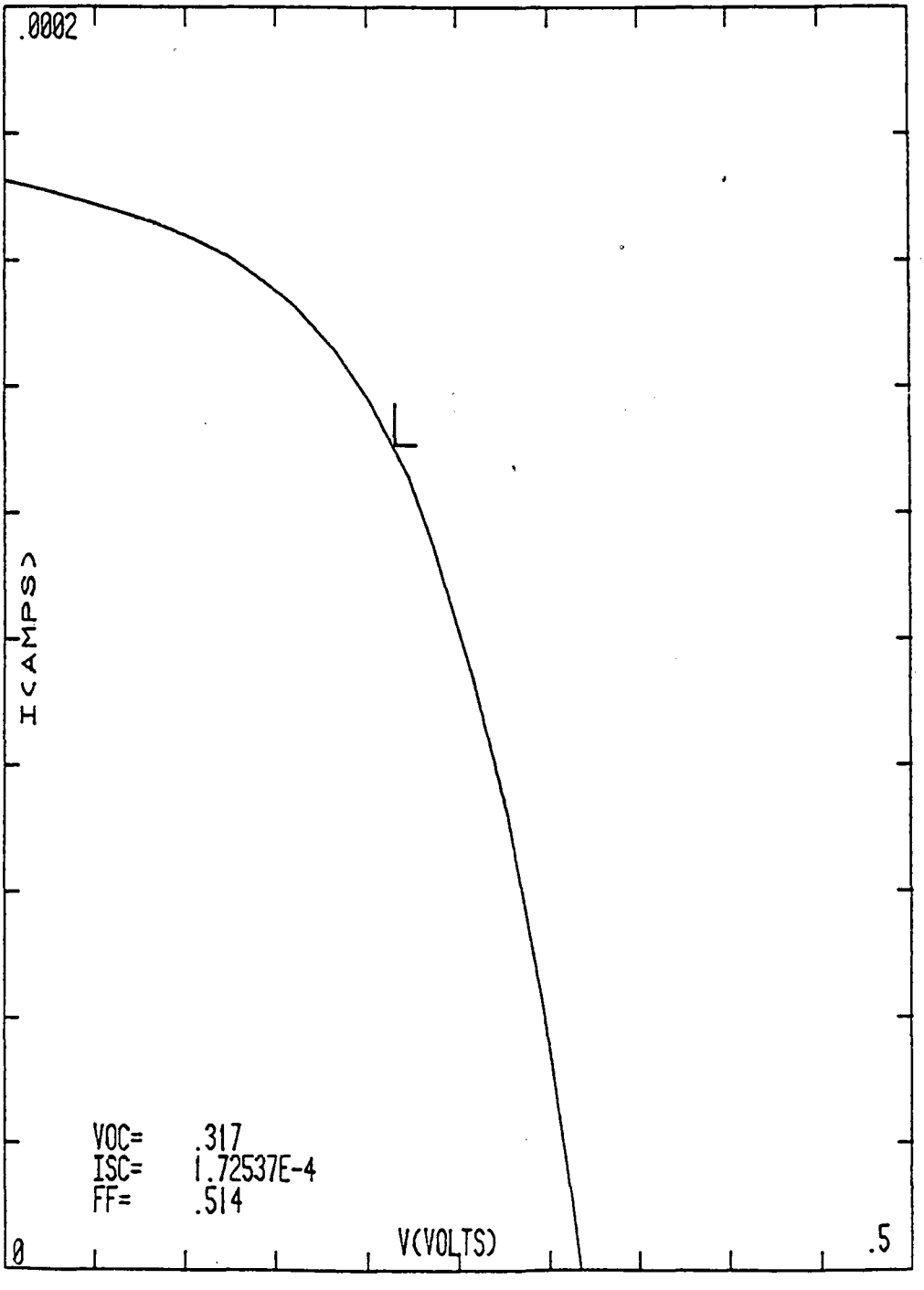

Fig. 4.5 Light I-V curve for the same cell as in Fig. 4.4 under simulated 1 SUN AM1 illumination.

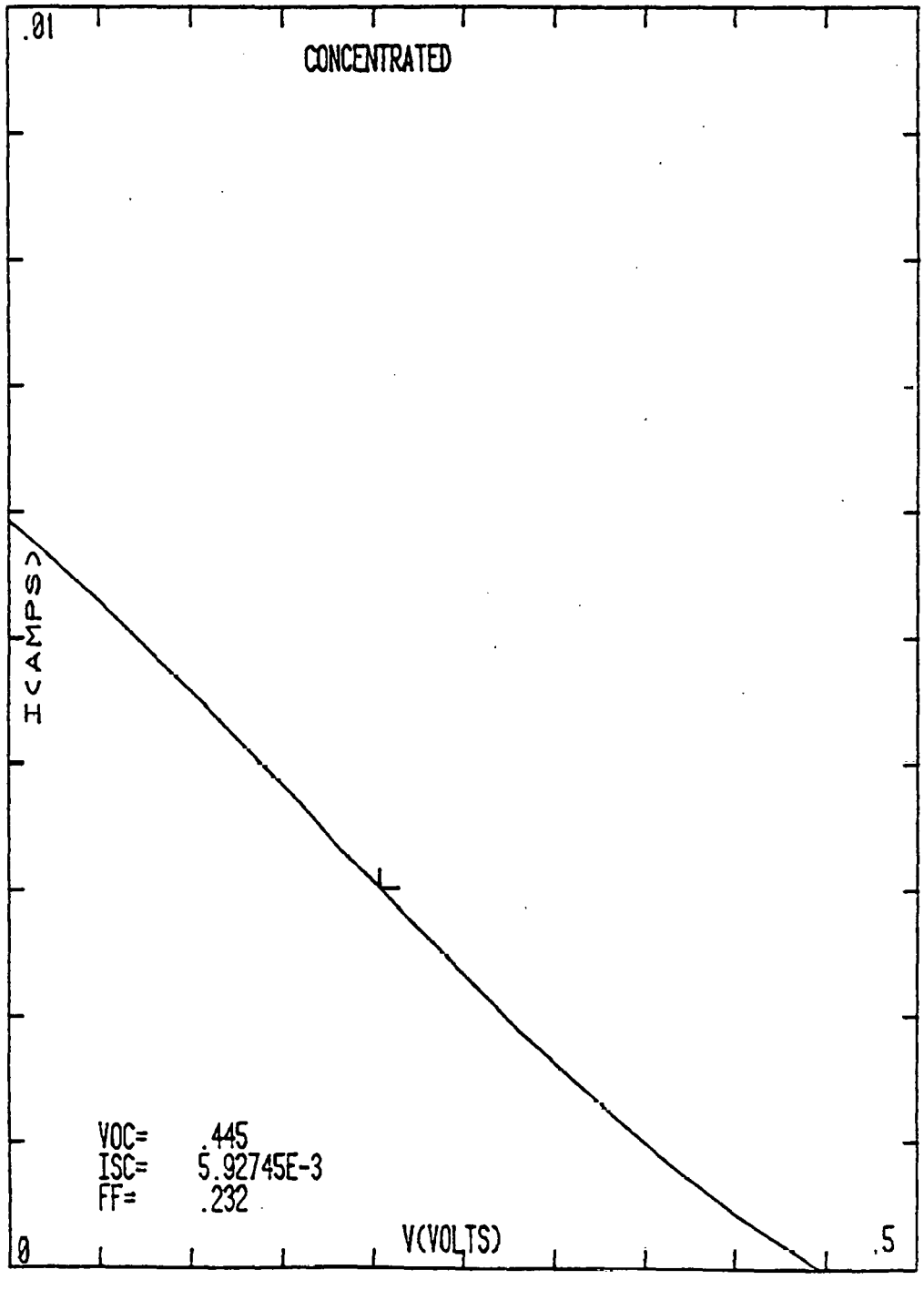

Fig. 4.6 Light I-V curve for the same cell as in Fig. 4.4 under simulated 35 SUNs AM1 illumination.

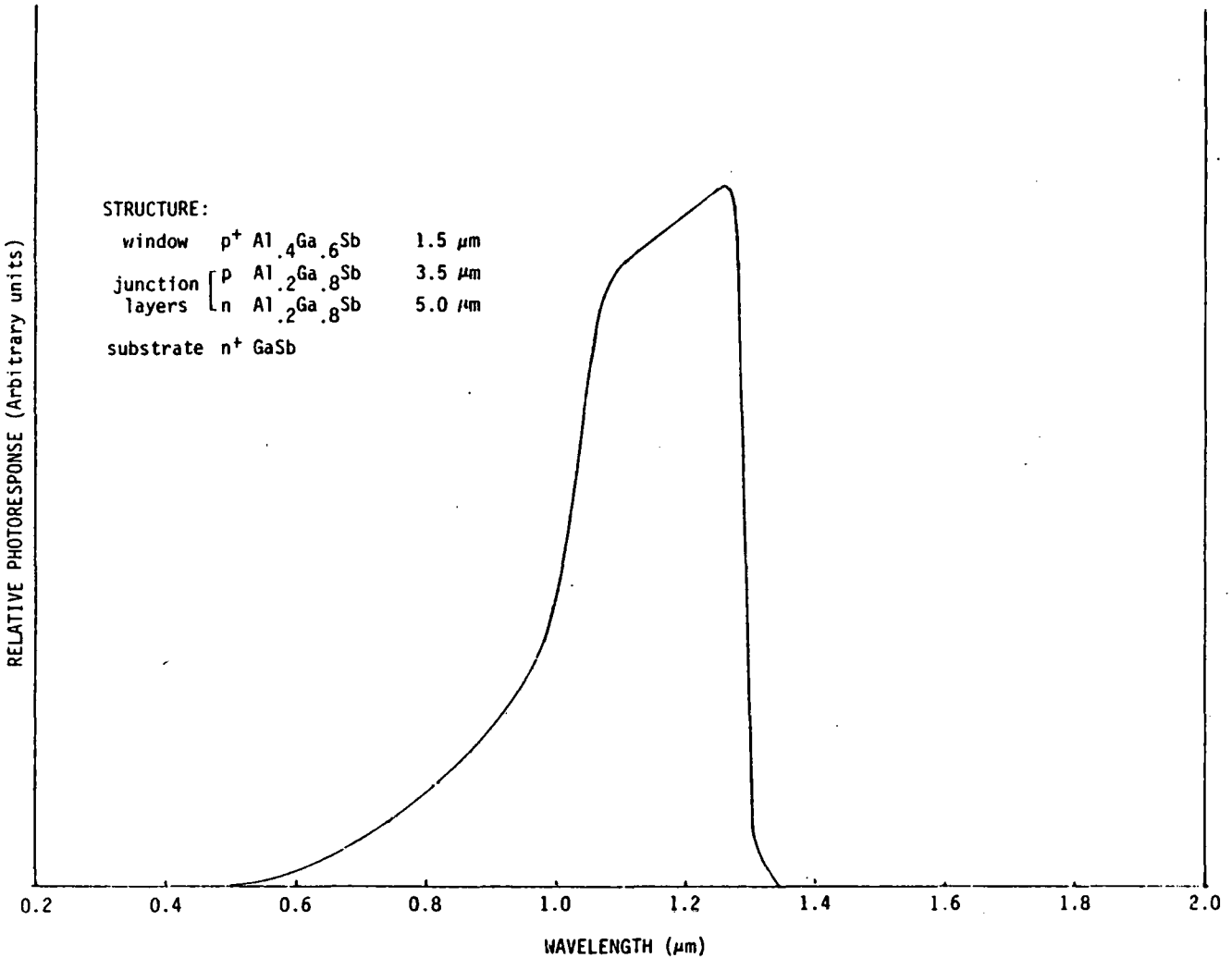

Fig. 4.7 Relative spectral response curve for the same cell as in Fig. 4.4

4.2.3 Measurements on Bonded Assemblies

Preliminary I-V measurements across bonded assemblies consisting of n-GaAs/in-situ formed AlSb/n-GaSb consistently show ohmic behavior for these structures. More detailed electrical and optical measurements will be reserved for subsequent assemblies currently being fabricated which contain AlGaAs and AlGaSb p-n junctions of the type to be used in the complete two junction converter.

5.0 REFERENCES

1. E. D. Jackson, Trans. Conf. on the Use of Solar Energy, Tucson, 1955, U. of Arizona Press, Tucson, Vol. 5, p. 122-126, 1958.

2. J. J. Loferski, 12th IEEE PV Spec. Conf. Proc., p. 957 (1976).

3. N. S. Alvi, C. E. Backus, G. W. Masden, 12th IEEE PV Spec. Conf. Proc., p. 948 (1976).

4. Kim Mitchell, 12th IEEE PV Spec. Conf. Proc., p. 529 (1976).

5. (a) Papers in 13th IEEE PV Spec. Conf. Proc. Session IX-B, Basic Studies: Tandem Cells, p. 853 ff., (1978).
(b) Papers in 30 Percent Device Section, NASA Conf. Publ. 2097, Proc. of Conf. on Solar Cell High Efficiency and Radiation Damage, NASA Lewis Research Center, Cleveland, Ohio, June 13-14 (1979), p. 255 ff.

6. L. W. James and R. L. Moon, Appl. Phys. Lett. 26, 467 (1975).

*U.S. GOVERNMENT PRINTING OFFICE: 1980-640-268/285